Published in final edited form as:
DNA Repair (Amst). 2007 November ; 6(11): 1629–1641.

Human endonuclease VIII-like (NEIL) proteins in the giant DNA Mimivirus

Viswanath Bandaru[1], **Xiaobei Zhao**[2], **Michael R. Newton**[2], **Cynthia J. Burrows**[2], and **Susan S. Wallace**[1,*]

1 *Department of Microbiology and Molecular Genetics, The Markey Center for Molecular Genetics, The University of Vermont, Stafford Hall, 95 Carrigan Drive, Burlington, Vermont 05405-0068*

2 *Department of Chemistry, University of Utah, 315 South 1400 East, Salt lake City, Utah 84112-0850*

Abstract

Endonuclease VIII (Nei), which recognizes and repairs oxidized pyrimidines in the Base Excision Repair (BER) pathway, is sparsely distributed among both the prokaryotes and eukaryotes. Recently, we and others identified three homologs of *E. coli* endonuclease VIII-like (NEIL) proteins in humans. Here, we report identification of human NEIL homologs in Mimivirus, a giant DNA virus that infects *Acanthamoeba*. Characterization of the two mimiviral homologs, MvNei1 and MvNei2, showed that they share not only sequence homology but also substrate specificity to the human NEIL proteins, that is, they recognize oxidized pyrimidines in duplex DNA and in bubble substrates and as well show 5′2-deoxyribose-5-phosphate lyase (dRP lyase) activity. However, unlike MvNei1 and the human NEIL proteins, MvNei2 preferentially cleaves oxidized pyrimidines in single stranded DNA forming products with a different end chemistry. Interestingly, opposite base specificity of MvNei1 resembles human NEIL proteins for pyrimidine base damages whereas it resembles *E. coli* formamidopyrimidine DNA glycosylase (Fpg) for guanidinohydantoin (Gh), an oxidation product of 8-oxoguanine. Finally, a conserved arginine residue in the “zincless finger” motif, previously identified in human NEIL1, is required for the DNA glycosylase activity of MvNeil. Thus, Mimivirus represents the first example of a virus to carry oxidative DNA glycosylases with substrate specificities that resemble human NEIL proteins. Based on the sequence homology to the human NEIL homologs and novel bacterial NEIL homologs identified here, we predict that Mimivirus may have acquired the DNA glycosylases through the host-mediated lateral transfer from either a bacterium or from vertebrates.

Keywords

Mimivirus; endonuclease VIII-like; oxidative DNA damage; human NEIL1

1. Introduction

All organisms are equipped with DNA glycosylases to repair oxidative DNA damage caused by reactive oxygen species (ROS) generated during endogenous metabolism and from exposure

Address correspondence to: Susan S. Wallace, Department of Microbiology and Molecular Genetics, The Markey Center for Molecular Genetics, The University of Vermont, Stafford Hall, 95 Carrigan Drive, Burlington, Vermont 05405-0068, Tel. (802) 656-2164; Fax: (802) 656-8749; E-mail: susan.wallace@uvm.edu.

to ionizing radiation. In *Escherichia coli*, three different DNA glycosylases namely formamidopyrimidine DNA glycosylase (EcoFpg), endonuclease VIII (EcoNei) and endonuclease III (EcoNth) recognize and excise various oxidative lesions (for reviews see [1–3]). Both endonucleases III and VIII show broad specificity for pyrimidine base damages such as urea, thymine glycol (Tg), 5-hydroxycytosine (5OHC), 5-hydroxyuracil (5OHU) and ring saturation products of thymine and uracil [5, 6-dihydrothymine (DHT) and 5, 6-dihydrouracil (DHU)] [1–3]. On the other hand formamidopyrimidine DNA glycosylase (EcoFpg) recognizes mainly 8-oxoguanine (8-oxoG) and formamidopyrimidine derivatives of 'A' (FapyA) and 'G' (FapyG) [4]. More recently it has been shown that due to its low redox potential, 8-oxoG can undergo further oxidation to yield ring-opened products, spiroiminodihydantoin (Sp) and guanidinohydantoin (Gh) [5–8]. These lesions are highly mutagenic and result in G→T and G→C transversion mutations [9,10]. All three *E. coli* DNA glycosylases recognize and cleave Sp and Gh lesions in duplex DNA [11,12]. Although *E. coli* Fpg and Nei differ in their primary substrate specificities, they both share common DNA binding structural motifs, the helix-two-turns-helix (H2TH) and the zinc finger motif [13,14].

Among the three aforementioned DNA glycosylases in *E. coli*, endonuclease III (Nth) is the most widely distributed across all three domains i.e. bacteria, eukaryotes and archaea with multiple paralogs in some actinobacteria, *Deinococcus* and *Entamoeba histolytica* (unpublished observations). Homologs of *E. coli* Fpg are restricted mainly to bacteria and have not been identified in eukaryotes and archaea with the exception of plants, some filamentous fungi and an uncultured methanogenic archaeon. Instead, 8-oxoguanine DNA glycosylase (Ogg), a functional homolog of *E. coli* Fpg is the primary DNA glycosylase that removes 8-oxoguanine in eukaryotes and in archaea. In contrast, endonuclease VIII (Nei) is less commonly found in bacteria and in eukaryotes and until recently, the only Nei protein characterized was endonuclease VIII from *E. coli* [15]. The first eukaryotic homologs of *E. coli* Nei designated NEIL1, NEIL2 and NEIL3 (Nei-Like) were recently identified in humans and NEIL1 and NEIL2 extensively characterized [16–20]. All three NEIL paralogs have been identified in the sequenced genomes of other eukaryotic vertebrates.

Unlike cellular organisms, DNA repair proteins are not very well conserved in viruses presumably due to their small genomes. An exception to this rule is the recently discovered Mimivirus, a double stranded DNA virus that infects *Acanthamoeba polyphaga*. First isolated from the cooling tower water suspected of causing a pneumonia outbreak in Bradford, UK, the Mimivirus (short for "Mimicking microbe") is the largest known virus to date with a particle diameter of at least 400 nm and a genomic size of 1.2 megabases [21]. Sequencing of the mimiviral genome revealed some interesting features not previously identified in other viruses. Of the 1262 putative ORF's identified, 911 encode proteins and 36 genes are unique to the Mimivirus [21]. Six of these unique genes were annotated as involved in the repair of alkylated DNA damage, mismatch repair, UV damage and oxidative DNA damage. In this paper, we report cloning of two of the mimiviral DNA repair genes (L315, L720) and detailed characterization of their encoded proteins (MvNei1, MvNei2) predicted to repair oxidized purines.

2. Materials and Methods

2.1 Cloning and purification of Mimiviral Nei proteins

Mimiviral genomic DNA, obtained from Dr. Didier Raoult (*Unité des Ricketssies*, Marseille, France), was used as template to amplify MvNei1 (L315) and MvNei2 (L720Δ43) by polymerase chain reaction. Both mimiviral genes were cloned into NdeI- XhoI sites of the pET22b expression vector (Novagen) to give C-terminal hexa-his tagged proteins. MvNei1 mutants (P2G and R277A), modifications of an internal NdeI restriction site and tandem repeats

of rare codons in MvNei2 were made using the QuickChange XL site-directed mutagenesis kit (Stratagene, La Jolla, CA).

Expression and purification of MvNei1 and MvNei2 were essentially the same as described for human NEIL1 [22]. Briefly, pET22b carrying MvNei1 or MvNei2 was induced in Rosetta (DE3) pLys (Novagen) with 1 mM IPTG at an OD_{600} of ~0.5 for 12–16 hr at 16°C. Cleared cell lysates were first loaded onto HiTrap Chelating HP column and later onto HiTrap SP FF using ÄKTA prime plus (Amersham Biosciences, Piscataway, NJ). After eluting from the second column, proteins were dialyzed into the storage buffer (20 mM Hepes 7.5, 150 mM NaCl, 1 mM EDTA, 1 mM DTT and 50 % glycerol), enzyme concentrations were determined by the Bradford assay and the enzymes stored at −20°C. The active fraction of the enzyme preparations was determined using the Schiff base assay [22].

All other DNA glycosylases used as controls in this paper were from our lab stocks prepared as described previously [22]. Human AP endonuclease (APEX) was purchased from Trevigen (Gaithersburg, MD).

2.2 DNA Glycosylase/lyase Assay

Oligonucleotides (35-mers) carrying various oxidative base damages, except Sp and Gh, were in the sequence 5′-TGTCAATAGCAAG**X**GGAGAAGTCAATCGTGAGTCT-3′ and were purchased from The Midland Certified Reagent Company, Midland, Texas. Spiroiminodihydantoin (Sp) and guanidinohydantoin (Gh) were synthesized in a 30-mer (5′-TGTTCATCATGCGTC**Y**TCGGTATATCCCAT-3′ and a 14–mer (5′-GCGTCCA**Z**GTCTAC -3′) oligonucleotides respectively as described previously [23]. All oligonucleotides were purified either on a PAGE gel or by HPLC prior to use.

For the assays, 1 pmole of damage-containing oligonucleotide was 5′-end labeled with T4 polynucleotide kinase and [α-^{32}P] dATP, stopped with 50 mM EDTA and ethanol precipitated to remove unincorporated radionucleotide. To minimize errors due to loss from ethanol precipitation, the labeled oligonucleotide was diluted 10-fold with the corresponding unlabeled damaged oligonucleotide and used directly as single stranded DNA or annealed with 10 pmoles of complementary oligonucleotide in a 40 μl reaction containing 10 mM Tris (pH 8.0) and 50 mM NaCl. For making substrates containing an AP site, single or double stranded 35-mer oligonucleotides containing uracil (U) were prepared as described above, treated with 2 U of *E. coli* uracil DNA glycosylase (New England Biolabs, Beverly, MA) at 37°C for 30 min, ethanol precipitated and resupended in 40 μl of 10 mM Tris pH 8.0 and 50 mM NaCl. All DNA glycosylase/lyase activity assays were setup as described below unless otherwise noted. In a 10 μl reaction, various double stranded substrates were incubated with either control enzymes (EcoNth, EcoNei, hNEIL1, hOGG1, EcoFpg) or increasing concentrations of MvNei1 or MvNei2 in their respective assay buffers at 37°C for 30 min. The assay buffer for EcoNei, EcoFpg and EcoNth was 10 mM Tris pH 7.6, 100 mM NaCl, 1 mM EDTA; for hOGG1, 20 mM Tris pH 7.4, 100 mM NaCl, 0.15 mg/ml BSA; for NEIL1, 20 mM Ches-KOH pH 9.5, 100 mM NaCl, 1 mM EDTA; for MvNei1, 20 mM Hepes-KOH pH 7.8, 75 mM KCl, 1 mM EDTA, 1mM $MgCl_2$, 0.1 mg/ml BSA; for MvNei2, 20 mM Tris pH 8, 100 mM NaCl. Since all enzymes were diluted in their respective storage buffers containing 50 % glycerol, the final glycosylase reactions also contained 5% glycerol. Reactions were terminated with equal volumes of formamide dye, heated and loaded onto 12 % denaturing polyacrylamide gel. Wherever necessary, the load volumes were normalized to radioactive counts for qualitative comparisons.

For kinetic analysis with MvNei1, 0.3 nM active enzyme was incubated with 1–10 nM Tg:A substrate in a 100 μl reaction and 5–15 nM of Gh:C or Gh:A in 50 μl reaction containing MvNei1 assay buffer at 37°C. At various time intervals (30 s to 80 min), aliquots of the reaction were terminated with equal volumes of formamide dye, heated, loaded onto a 12% denaturing

polyacrylamide gel and quantified using Quantity-One (Bio-Rad). Dynafit was used to calculate kinetic parameters by least square regression globally of experimental data plotted as time versus product formed.

2.3 dRP Lyase Assay

The substrate for the dRP lyase assay was prepared essentially as described by Garcia-Diaz *et al*. [24]. A uracil-containing oligonucleotide (35-mer) with the same sequence context used for DNA glycosylase assays described above was employed to make a 22-mer substrate with a 5′ 2 deoxyribose-5-phosphate (5′-dRP) moiety opposite 'G'. A 10 μl reaction containing 50 mM Hepes pH 7.5, 20 mM KCl, 2 mM DTT, 10 mM $MgCl_2$ and 100 fmoles of human AP endonuclease (APEX)-treated AP:G substrate was incubated with DNA glycosylases or human DNA polymerase β (Trevigen, Gaithersburg, MD) as indicated in the Fig. 3 Legend. Following incubation at 37°C for 30 min, the reactions were chilled on ice and treated with 340 mM sodium borohydride ($NaBH_4$) for 20 minutes on ice. Subsequently, the reactions were ethanol precipitated, resuspended in 10 μl formamide dye and loaded onto 20 % denaturing polyacrylamide gel.

2.4 Assays with bubble substrates

The oligonucleotides and the procedure used to make duplex substrates containing various size bubbles were same as described by Dou *et al*. [25]. Annealing Reactions (40 μl) containing oligonucleotides in 10 mM Tris (pH 8.0) and 50 mM NaCl were heated in boiling water for 3 min and slow cooled for ~ 1 hr. Glycosylase reactions with MvNei1 and different bubble substrates were performed as described above.

3. Results

3.1 Identification of Fpg/Nei family members in Mimivirus

The sequence of the giant DNA Mimivirus was recently completed and fully annotated by Raoult *et al*. [21]. They compared the mimiviral putative open reading frames (ORF's) with the Cluster of Orthologous Groups (COG's) database and reported L315 and L720, as DNA repair proteins involved in hydrolysis of DNA containing ring-opened N7-methylguanine (Fapy-7-MeGua), a substrate for *E. coli* formamidopyrimidine DNA glycosylase (EcoFpg). Also, a PSI-BLAST search with human NEIL1 identified, albeit with low E-values, the two mimiviral L315 and L720 proteins showing similarity to the human NEIL1 protein. Further, a BLAST search of all sequenced microbial genomes with mimiviral L720 identified two homologs in *Psychroflexus torquis* (PtoNei) and

3.2 Zymomonas mobilis

(ZmoNei) with ~30 % identity to the L720 sequence. We aligned the L315, L720, PtoNei and ZmoNei sequences with representative members of Fpg/Nei family including homologs from an archaeon, *Candida albicans* and *Arabidopsis thaliana* (Fig. 1). Initial attempts to align the reported L720 sequence were unsuccessful however visual inspection of the protein sequence showed an N-terminal extension of 43 amino acids from an internal methionine next to the catalytic residues important for the DNA glycosylase/lyase activity of Fpg/Nei family members. We surmised that the authentic N-terminus of the second mimiviral Fpg/Nei homolog should start 43 amino acids away from the predicted N-terminus in the reported L720 sequence. Therefore, L720 with the N-terminal extension of 43 residues deleted (L720Δ43) was used for sequence alignments and for the biochemical characterization described below. At the N-terminus, mimiviral L315, PtoNei and ZmoNei carry the catalytic proline residue whereas in L720Δ43 the proline is replaced by a valine (Fig. 1). Also the third glutamic acid residue important for the DNA glycosylase activity is present in all four sequences. The DNA

binding helix-two-turns-helix (H2TH) motif is conserved with the exception of a glycine insertion in L315. At the C-terminus, the cysteines that coordinate zinc to form a β-hairpin loop of the zinc finger domain are present in L720Δ43 and ZmoNei but are missing in L315 and PtoNei sequences. Furthermore, the mimiviral L720Δ43 and ZmoNei carry the CHCC type zinc finger and a glycine residue is inserted between the cysteine and histidine residues in the zinc finger (Fig. 1). Finally, an arginine residue conserved in the zinc finger domain of all Fpg/Nei family members is also found in L315, L720, PtoNei and ZmoNei sequences.

3.3. Cloning and Purification of mimiviral L315 and L720Δ43

The Fpg/Nei family members utilize proline at the amino terminus to initiate the removal of the damaged base i.e. DNA glycosylase activity, by cleaving the N-glycosylic bond between the sugar and the damaged base. This would necessitate correct processing of the N-terminal formyl-methionine (f-Met) and the use of C-terminal tags only. The full length L315 and L720Δ43 were cloned into a pET vector, expressed and purified essentially as described for human NEIL1 [16]. Both C-terminal hexa-his tagged L315 (34.5 kDa) and L720Δ43 (33.5 kDa) were purified to homogeneity and the N-terminal sequence was verified by Edmund degradation. These results showed that the N-terminal methionine was completely processed in L315 preparation whereas approximately half of the L720Δ43 protein retained the initiator methionine (data not shown). The extent of N-terminal methionine excision by *E. coli* methionine aminopeptidase (MetAP) is determined by the penultimate residue and a valine at the second position results in partial or incomplete processing of the initiator methionine in the proteins expressed in *E. coli* [26,27]. In this case, L720Δ43 has a valine in the second position (Fig. 1) and hence showed incomplete removal of N-terminal methionine in the protein preparation. Nevertheless, we used purified L720Δ43 protein for a qualitative comparison of the substrate specificities with mimiviral L315 protein.

3.4 Specificity of L315 and L720Δ43 for duplex substrates

To test the DNA glycosylase/lyase activities, purified L315 and L720Δ43 proteins were incubated in equimolar ratios with substrates carrying different purine and pyrimidine lesions. These initial experiments showed that the mimiviral L315 and L720Δ43 proteins recognize and cleave pyrimidine lesions (data not shown). Since oxidized pyrimidines and not 8-oxoguanine are the primary substrates for both the proteins, we designated Mimiviral L315 as MvNei1 and L720Δ43 as MvNei2. Optimal DNA glycosylase assay conditions were determined for MvNei1 and MvNei2 using duplex substrates containing thymine glycol (Tg) and 5-hydroxyuracil (5OHU), respectively. Both MvNei1 and 2 showed activities over a broad pH range with optima at pH 7.8 and 8.0 respectively (data not shown). Also maximal activities of MvNei1 and MvNei2 were observed in 75 mM KCl and 100 mM NaCl respectively. Addition of BSA or Mg^{2+} did not influence the activity of MvNei2 but slightly improved the activity of MvNei1 (data not shown).

Under optimized reaction conditions, purified MvNei1 and 2 were assayed for their preference for various purine and pyrimidine base damages in duplex DNA. Excess enzyme over substrate was used in order to rule out dissociation constant (K_d) as a determinant for the substrate specificity. Also a double stranded substrate with an abasic site (AP) was used to test the lyase activity i.e. ability to cleave the phosphodiester backbone. Bifunctional human 8-oxoguanine DNA glycosylase (hOGG1), EcoNth, EcoFpg and EcoNei were used as controls to ascertain the end chemistry of products formed in the glycosylase reactions with MvNei1 and MvNei2. Specifically, hOGG1 and EcoNth cleave the phosphodiester backbone via β-elimination mechanism to give products with a 3′α, β-unsaturated aldehyde whereas EcoNei and EcoFpg leave a terminal 3′phosphate via β, δ-elimination mechanism. As shown in Fig. 2A & B, both MvNei1 and 2 recognize pyrimidine lesions especially thymine glycol, 5-hydroxyuracil (5OHU), and to a lesser extent, 5-hydroxycytosine (5OHC) while both showed weak activity

on 8-oxoG even at 10-fold excess enzyme over substrate. A notable difference between MvNei1 and human NEIL1, and MvNei2 is that MvNei2 cleaved the DNA backbone primarily via β-elimination although products resulting from β, δ-elimination were observed to a lesser extent (Fig. 2B). MvNei1 and 2 also showed efficient lyase activity when incubated with an abasic site in duplex DNA (Fig. 2C). At lower concentrations of MvNei2, the lyase reaction on an AP substrate yielded mainly β-elimination products whereas β, δ-elimination products were observed with 10-fold excess MvNei2 over substrate (Fig. 2C). Finally, MvNei1 and 2 showed no detectable activity on single stranded DNA with a uracil and double stranded DNA with mismatches (U:C, T:G) even in enzyme excess over substrate (data not shown).

Although 8-oxoguanine (8-oxoG) is a poor substrate for NEIL1 and EcoNei, they both recognize and cleave spiroiminodihydantoin (Sp) and guanidinohydantoin (Gh) damages [12,28]. Therefore, we tested the activities of MvNei1 and MvNei2 on Gh and Sp damages in duplex DNA. MvNei2 showed only weak activity on double stranded Sp:C and Gh:C whereas these are good substrates for MvNei1 and human NEIL1 (Fig. 2D).

3.5 dRP lyase activity of MvNei1 and MvNei2

A characteristic feature of Fpg/Nei family members is their ability to remove the 5′-dRP moiety generated from incision at abasic sites by human AP endonuclease (APEX) [15,29]. To demonstrate this activity in the mimivirus homologs, a 5′dRP-containing 22-mer substrate was incubated with human NEIL1, MvNei1 and MvNei2. Human DNA polymerase β (hPolβ) which possesses dRP lyase activity also served as a control for the assay. As shown in Fig. 3, both MvNei1 and MvNei2 processed the 5′-dRP moiety to give a 22-mer product.

3.6 Activities of MvNei1 and MvNei2 on damage-containing single stranded and bubble substrates

Human NEIL1 and NEIL2 cleave 5-formyluracil (5-foU), 5-hydroxyuracil (5OHU), 5-hydroxymethyl uracil (5hmU) when present in single stranded DNA [30]. Also mouse Neil1 recognizes thymine glycol, spiroiminodihydantoin (Sp) and guanidinohydantoin (Gh) in single stranded oligonucleotides [28]. To test the specificities of MvNei1 and MvNei2 for single stranded oligonucleotides carrying Sp and Gh, we used equimolar ratios of enzyme to substrate. Human NEIL1, MvNei1 and MvNei2 cleaved abasic sites (AP) and pyrimidine base damages but showed only weak activity on 8-oxoG in single stranded DNA (Fig. 4A). As we observed with duplex substrates, MvNei2 cleaved pyrimidine base damages in single stranded DNA by β-elimination (Fig. 4A). On the other hand, Gh and Sp lesions in single stranded DNA were poor substrates for hNEIL1 and MvNei1 whereas MvNei2 cleaved both damages although Sp was cleaved better than Gh in single stranded DNA (Fig. 4B).

In addition to cleaving damaged bases by a different mechanism i.e. primarily β-elimination, MvNei2 prefers base damages in single stranded DNA more than in double stranded DNA. This inference was based on the observation that MvNei2 cleaved oxidative lesions in single stranded DNA more readily at equimolar ratios than in duplex DNA with excess enzyme over substrate (compare Fig. 2B and Fig. 4). To test this hypothesis, we incubated Sp lesions in single and double stranded DNA with 2 to 10-fold excess MvNei2 over substrate (Fig. 5). At higher concentrations of MvNei2, a double strand-specific exonuclease appeared to remove the 5′ radioactive label on both the substrate and product bands. Nevertheless, comparing the amount of cleaved substrate at lower enzyme concentrations, it is evident that MvNei2 prefers the Sp damage in single stranded DNA compared to duplex DNA (Fig. 5).

As mentioned earlier, incomplete processing of the N-terminal methionine gave partially active MvNei2 and hence it could not be used for the quantitative comparisons described below. Although MvNei1 and human NEIL1 recognize all the pyrimidine base damages in duplex

DNA, both enzymes prefer Tg, 5OHC and 5OHU damages in single stranded DNA (Fig. 4). To determine the preferred single stranded substrate for MvNei1, human NEIL1 and MvNei1 were incubated with varying amounts of lesion-containing single stranded substrates (Fig. 6). These experiments showed that under multiple turnover conditions, 5OHU in single stranded DNA is the best substrate for both human NEIL1 and MvNei1.

Human NEIL1 and NEIL2 were previously shown to recognize oxidative base damages, specifically 5OHU and 8-oxoG in bubble substrates [25]. Since MvNei1 recognizes base damages in single stranded DNA and shares sequence homology to human NEIL1, we tested the activity of MvNei1 on 5OHU-containing bubble substrates. Duplex substrates (51-mer) with 5OHU placed in the middle of the bubbles were made as described by Dou *et al* [25] and the secondary structure was verified by their mobility on a 10% native PAGE gel. Single stranded DNA migrated faster than the duplex DNA while the bubble substrates migrated more slowly than duplex DNA and this shift in mobility increased as a function of the bubble size from 5–19 nucleotides (Fig. 7A). Next, we incubated bubble substrates (B5, B11 and B19), single stranded and duplex DNA with MvNei1 in order to determine the specificity under conditions of excess substrate. As shown in Fig. 7B, MvNei1 cleaved 5OHU in all three bubble substrates but showed ~ 4 to 6 fold higher activity on 5OHU-B5 and single stranded DNA compared to 5OHU in a 11 or 19 nucleotide bubble substrate. Nonetheless, MvNei1 preferred 5OHU in double stranded DNA rather than in single stranded DNA or in bubble substrates (Fig. 7B).

All pyrimidine base damages as well as Sp and Gh are substrates for MvNei1 (Fig. 2A and D) especially when present in duplex DNA (Fig. 7B). To determine the relative rates of incision, MvNei1 was incubated with Sp, Gh and pyrimidine damage-containing duplex DNA molecules under multiple turnover conditions. As shown in Fig. 8, oxidation products of 8-oxoguanine especially Sp opposite a ‘C’ are the preferred substrates for MvNei1. Among pyrimidine lesions, thymine glycol is the best substrate whereas the ring-saturated DHU and DHT are relatively poor substrates for MvNei1 (Fig. 8).

During DNA replication, DNA polymerases incorporate an ‘A’ or a ‘C’ opposite 8-oxoguanine and *in vitro, E. coli* exonuclease deficient Klenow fragment incorporates an ‘A’ or ‘G’ opposite Sp or Gh damages [9,23]. Since 8-oxoG oxidation products are good substrates for MvNei1 and the intercalation loop of MvNei1 that interacts with the estranged base resembles that of EcoFpg and not EcoNei [13,31], we checked the opposite base specificity of MvNei1 for Gh and Sp when paired with A, T, G and C in duplex DNA. Also for comparison, we tested the MvNei1 base specificity opposite Tg, 5OHU and 5OHC damages. As shown in Fig. 9A, MvNei1 cleaved Tg efficiently with little or no preference for the opposite base in the complementary strand. Similar results of weak opposite base specificity were also observed with other pyrimidine damages, 5OHU and 5OHC (data not shown). MvNei1 also cleaved Sp efficiently opposite all 4 bases, although the cleavage rate was faster with a ‘C’ compared to an ‘A’ in the complementary strand (data not shown). On the other hand, MvNei1 showed strong opposite base specificity for Gh in duplex DNA. Specifically, MvNei1 cleaved Gh:C substrate readily whereas slow cleavage of Gh was observed when paired with an ‘A’ in double stranded DNA (Fig. 9B). This is a biological anomaly given that MutY does not remove A opposite Gh [11].

Next, we determined kinetic parameters of MvNei1 for Gh opposite a ‘C’ or an ‘A’ as well as with Tg:A substrates (Table 1). The active enzyme fraction in the MvNei1 preparation was estimated by Schiff base assay and was found to be 30% active (data not shown). The substrate concentrations used to determine the kinetic parameters were within the linear range of enzyme activity. As shown in Table 1, although the Km’s are comparable, the catalytic turnover of MvNei1 was ~ 13-fold higher for Gh:C than for Tg:A under steady state conditions. On the

other hand, MvNei1 showed specificity for the opposite base mainly due to the K_m for the substrate. Specifically, MvNei1 showed a ~1000-fold higher K_m for Gh when paired with an 'A' compared to a 'C' opposite the lesion.

3.7 Activity of MvNei1 mutants

The conserved proline and arginine residues at positions 2 and 277 respectively were mutated to demonstrate the role for these residues in the DNA glycosylase/lyase activity of MvNei1. The P2G and R277A MvNei1 mutants were constructed, expressed and purified as described for wild type MvNei1. Purified enzymes were incubated with Tg:A substrate and an abasic site in duplex DNA to test the bifunctional DNA glycosylase/lyase and the lyase activities of MvNei1 mutants. As shown in Fig. 10A, mutation in the N-terminal raline residue of MvNei1 abolished the DNA glycosylase activity on Tg:A but showed reduced lyase activity on an AP:G substrate. On the other hand, a R277A mutation in MvNei1 resulted in decreased bifunctional activity on Tg:A substrate (Fig. 10B) but did not affect the lyase activity of the mutant (data not shown).

4. Discussion

4.1 Mimivirus and DNA Repair

In this paper, we report characterization of two DNA repair enzymes in the giant DNA Mimivirus as DNA glycosylases that recognize and repair oxidized pyrimidines. Although DNA glycosylases, namely the T4 pyrimidine dimer (T4-Pdg) and uracil DNA glycosylases (Udg), have previously been identified in DNA viruses that belong to Myoviridae (T4, RB69), Phycodnaviridae (chlorella), Herpesviridae (simplex) and poxviridae (vaccinia) families, the mimiviral MvNei1 and MvNei2 represent the first examples of oxidative DNA glycosylases in a virus [32,33]. Additionally, Mimivirus also encodes uracil DNA glycosylase (Udg), endonuclease IV (Nfo), O^6-methylguanine-DNA-methyltransferase (Mgmt), 1-methyladenine-DNA-dioxygenase (AlkB), UV endonuclease (UvdE) and DNA mismatch repair (MutS) proteins [21].

Mimivirus is a nucleocytoplasmic DNA virus (NCLDV) and a two stage life cycle has been proposed that involves early replication in the nucleus where viral DNA is synthesized and late replication in the cytoplasm of the host *Acanthamoeba polyphaga* [34]. Recent analysis of the non-coding region of the mimiviral genomic DNA identified a conserved promoter sequence motif, AAAATTGA upstream of ~50 % of the mimiviral genes [35]. Except for the AlkB and Mgmt homologs, all other mimiviral DNA repair genes, including MvNei1 and MvNei2, lack this octamer sequence in the upstream promoter region. It has been suggested that genes with this TATA-box like octamer motif could be transcribed in host cytoplasm whereas genes missing this sequence motif may be expressed in the host nucleus presumably from different viral promoter sequences [35]. Also, proteomic analysis identified 114 proteins in the mimiviral particles[36]. Of the various DNA repair proteins in Mimivirus, UV endonuclease (UvdE) but not the two oxidative DNA glycosylases is packaged in the virions [36]. Taken together, the data suggest that MvNei1 and MvNei2 may be required for repairing base damages during viral DNA synthesis in the nucleus of the amoeba.

4.2 Origin of the oxidative DNA glycosylases in Mimivirus

It is unlikely that the mimiviral oxidative DNA glycosylases were horizontally transferred from its host *Acanthamoeba polyphaga* for several reasons. First, 40% of the mimiviral proteins including the MvNei proteins show sequence similarity to homologs from other organisms whereas they show less than 1% match to a related protist, *Entamoeba histolytica* and to the EST database of *Acanthamoeba castellanii*, a close relative of mimiviral host [37]. Genes with the upstream octamer motif flank MvNei1 and MvNei2 in the mimiviral genome and a search

for the octamer motif in the partially sequenced *A. castellanii* genomic DNA revealed that this promoter-like sequence is less prevalent in the amoeba [35]. Further, Mimivirus preferentially uses A+T rich codons in contrast to its host relative *A. castellanii*, which uses mostly G+C rich codons [21].

Free-living *Acanthamoebae* feed on bacteria, fungi and algae by phagocytosis. Some of these ingested microorganisms are resistant to digestion and are capable of colonizing as symbionts in the host cytoplasm [38]. Pathogenic and non-pathogenic bacteria have been identified that can survive in *Acanthamoeba* and include Actinobacteria (*Mycobacterium avium, Mycobacterium leprae*), Bacteroidetes (*Flavobacterium sp*), Chlamydiae (*Chlamydophila pneumoniae*), Bacilli (*Listeria moncytogenes*) and Proteobacteria [*Bradyrhizobium japonicum* (α), *Burkholderia cepacia* (β), *Vibrio cholerae* (γ) and *Helicobacter pylori* (ε)] [38]. Mimivirus can infect all *Acanthameoba* species and enters the host cytoplasm after internalization by phagocytosis [34,39]. Therefore, it is possible that coexistence of Mimivirus and a bacterium in the cytoplasm of *Acanthamoeba* could provide a venue for gene transfer between them. In this regard, 15 % of mimiviral ORF's including MvNei1 and MvNei2 showed sequence matches to the genomic database of microbial environmental samples from the Sargasso Sea [40]. Also we identified Nei homologs in *Psychroflexus torquis* (PtoNei) and *Zymomonas mobilis* (ZmoNei) that belong to bacteroidetes and α-proteobacteria respectively. Although survival of these bacteria as endosymbionts in *Acanthameoba* is presently unknown, PtoNei and ZmoNei show sequence similarity to the mimiviral Nei proteins (Fig. 1). Alternatively, it is also plausible that the oxidative DNA glycosylases in Mimivirus were either acquired from or transferred to a higher eukaryote since the mimiviral host, *Acanthamoeba*, is an opportunistic pathogen in vertebrates including humans [41,42] and the mimiviral Nei proteins share sequence homology to the NEIL proteins in vertebrates (Fig. 1).

4.3 Similarities between Mimiviral Nei and human NEIL proteins

Sequence alignments of mimiviral Nei proteins with the representative Fpg/Nei homologs from bacteria, plants, fungi, archaea and humans identified a number of similarities between the human NEIL and mimiviral Nei proteins. At the C-terminus, all Fpg/Nei DNA glycosylase family members except human NEIL1 and its homologs carry four cysteines that coordinate a zinc atom to form β-hairpin motif observed in the crystal structures of liganded *E. coli* Nei and Fpg proteins [13,14,43]. Human NEIL1 and its homologs including MvNei1 instead carry an anti-parallel β-hairpin "zincless finger" motif first reported in the crystal structure of human NEIL1 [44]. A conserved arginine residue important for the DNA glycosylase activity (see below) and a threonine next to the arginine residue in the "zincless finger" motif are present in human NEIL1 and MvNei1 (Fig. 1). Similar "zincless finger" motifs with the conserved arginine and threonine residues are also found in bacteria (PtoNei), plants (AtFpg1) and fungi (CalNei).

On the other hand, it is remarkable that MvNei2 resembles human NEIL3 at the N-terminus and NEIL2 at the C-terminus. In fact a BLAST search with MvNei2 showed 23% identity to the N-terminus of the NEIL3 homolog in *Danio rerio* (Zebra fish) and 36% identity to the zinc finger region of the NEIL2 homolog in *Gallus gallus* (chicken). It is interesting that the N-terminal 43 amino acid extension in MvNei2 is annotated as a transmembrane region since the N-terminal residue is the nucleophile and requires a free amino terminus in all Fpg/Nei proteins. A similar N-terminal extension in front of the catalytic residues is also found in the *Canis familiaris* (dog) homolog of human NEIL3. The zinc finger in most Fpg/Nei proteins is of the C4 type whereas human NEIL2, ZmoNei and MvNei2 carry CHCC type zinc finger motif. This zinc finger motif was shown to coordinate a zinc atom and mutating the cysteines or histidine in human NEIL2 abolished DNA binding and enzymatic activity [45]. Finally, a glycine insertion between the cysteine and histidine residues in the zinc finger motif is present

in MvNei2, ZmoNei2 and human NEIL2 proteins demonstrating the conservation of the CHCC type zinc finger motif between viral, bacterial and human homologs respectively.

Besides sequence similarity, MvNei1 and MvNei2 also resemble NEIL family proteins in their substrate specificity for oxidized pyrimidines and further oxidation products of 8-oxoguanine. MvNei1 prefers Tg and 5OHU damages like human NEIL1 and cleaves them in duplex DNA with little or no opposite base specificity. The 8-oxoG oxidation products, Gh and Sp lesions are also substrates for mouse Neill [28] and human NEILl (unpublished observations). We show that human NEIL1 and MvNei1 recognize Gh and Sp when paired with a 'C' in duplex DNA. Unlike mouse NEIL1 which incises Gh and Sp efficiently when paired with all four bases, MvNei1 showed only weak specificity for the base across from the Sp lesion while the opposite base specificity for Gh resembles that of *E. coli* Fpg. Both EcoFpg and MvNei1 cleave Gh efficiently when paired with a 'C' and poorly when present across from an 'A' in the complementary strand. It is interesting that the best substrates for MvNei1 in double stranded DNA are Gh and Sp lesions but not 8-oxoG. Homologs of Fpg or Ogg have not been identified in a related protist, *E. histolytica* and therefore it is possible that Fpg/Ogg enzymes from endosymbiont bacteria repair 8-oxoG in *Acanthamoeba* and mimiviral genomes.

Like human NEIL2 [25], MvNei2 recognizes 5OHU in duplex DNA although oxidative lesions in single stranded DNA are the best substrates for MvNei2. All oxidative DNA glycosylases prefer base damages in double stranded DNA with the exception of human NEIL1 and NEIL2, which also recognize lesions in single stranded DNA and bubble substrates. It has been suggested that human NEIL proteins may be involved in repairing base damages in the DNA bubbles formed during transcription, replication or during remodeling of the chromatin DNA [25]. However, in the absence of the complementary strand, creation of strand breaks during removal of damaged bases in single stranded DNA could have deleterious consequences for the virus. It is possible that MvNei2 recognizes some other base damages in duplex DNA that are yet to be identified.

4.4 MvNei2 preferentially undergoes β-elimination

In the Fpg/Nei family members, the secondary amine of the N-terminal proline residue initiates a nucleophilic attack at the C1′ position of the nucleoside to cleave damaged substrates by a β, δ-elimination mechanism. Substituting the catalytic proline affects the bifunctional activities of all Fpg/Nei proteins as shown with MvNei1 (Fig. 10A). Based on this observation, it is reasonable to assume that MvNei2 should have diminished lyase activity and no DNA glycosylase activity since the N-terminal residue is a valine instead of a proline. However in the bacteriophage T4 pyrimidine dimer glycosylase (T4-Pdg), which is structurally unrelated to Fpg/Nei proteins, the primary amine (α-NH_2) of the N-terminal threonine residue is the nucleophile and cleaves the damaged substrate via a Schiff base intermediate [32]. Further, an internal glutamic acid residue in the T4-Pdg is required for stabilizing the imino intermediate (Schiff base) and for the formation of β-elimination products (Manuel et al 1995). Therefore, we predicted that the α-NH_2 of the N-terminal valine might serve as the nucleophile for the DNA glycosylase/lyase activity of MvNei2 on oxidized DNA damage-containing substrates. In support of this suggestion, a methionine substitution for proline reduced but did not eliminate the DNA glycosylase activity of *Candida albicans* Nei protein (unpublished observation). As noted with T4-Pdg, MvNei2 cleaved substrates carrying pyrimidine base damages and abasic sites in both duplex and single strand DNA via β-elimination (Fig. 4). The N-terminal valine residue may serve as the nucleophile but it is unlikely that the reaction mechanism of MvNei2 is similar to T4-Pdg mechanism since the α-NH_2 as the nucleophile can also cleave damaged substrates via β, δ-elimination as observed with the activities of MvNei1 P2G mutant on an AP:A substrate (Fig. 10A) and CalNei P2M mutant on DHU:G substrate (unpublished

observation). Hence the residue(s) responsible for the β-elimination mechanism of MvNei2 remains to be investigated.

4.5 The "zincless finger" in MvNeil

In addition to the H2TH motif, Fpg/Nei proteins use a zinc finger domain to bind in the minor groove of the DNA. A conserved arginine residue in the β-hairpin motifs of the human NEIL1 zincless finger and *E. coli* Nei zinc finger interacts with oxygens in the phosphate groups flanking the damage site. Substitutions of the arginine residue in human NEIL1 and *E. coli* Nei severely impair the DNA glycosylase but not the lyase activity of the enzymes [14] [44]. In the absence of a crystal structure and based on the sequence alignment, MvNei1 also carries a "zincless finger" motif similar to human NEIL1 since mutating the conserved arginine residue greatly reduced the DNA glycosylase but not the lyase activity of MvNei1 (Fig. 10B). Based on these observations, the archaeal Fpg with all four cysteines but missing the arginine residue in the zinc finger domain (Fig. 1) is expected to show weak DNA glycosylase activity on damage-containing substrates.

4.6 BER in viruses

The multi-step BER pathway in bacteria, archaea and eukaryotes includes DNA glycosylases, an apurinic/apyrimidinic (AP) endonuclease (APEX, endoIV), DNA polymerase (Pol I, Polβ) and a DNA ligase that are involved in the short-patch repair of oxidative DNA damages. Homologs of all BER proteins except the oxidative DNA glycosylases have been identified and characterized in African Swine Fever Virus (AFSV) [46,47]. The giant Mimivirus also carries all BER proteins including a recently characterized DNA ligase [48] and the two oxidative DNA glycosylases, MvNei1 and MvNei2 described in this paper.

A rate-limiting step in the BER pathway is the removal of 5′-dRP moiety resulting from incison of abasic sites by AP endonuclease [49]. The 5′-dRP moiety is processed by the associated dRP lyase activity of Fpg/Nei proteins in *E. coli* [15,29] whereas in eukaryotes, the 8 kDa N-terminal domain of the DNA polymerase β (pol β) removes the 5′-dRP moiety to leave a ligatable end [50]. Additionally, human NEIL proteins possess dRP lyase activity and may serve as back up for the pol β in human cells [51]. Like human NEIL proteins, MvNei1 and MvNei2 also showed dRP lyase activity (Fig. 3) suggesting a role in the viral BER pathway. Homologs of human Polβ have been identified in both ASFV and Mimivirus [21,46]. The ASFV polX missing the N-terminal 8-kDa domain is unlikely to exhibit dRP lyase activity whereas the mimiviral PolX carries the putative dRP lyase domain. The activities of other the mimiviral BER proteins remain to be investigated.

In summary, we have characterized two Fpg/Nei family homologs in a virus and shown them to have similar properties to the human NEIL proteins. Mimivirus is the first example of a virus encoding an oxidative base excision repair system from glycosylase to ligase and thus represents an excellent model system for further studies.

Acknowledgements

We thank Prof. Didier Raoult of *Unité des Ricketssies*, Marseille, France, for generously providing Mimiviral genomic DNA, Jeffrey Blaisdell for help with kinetic analysis, Alicia Holmes for technical assistance. We also wish to thank Prof. Sheila David (UC Davis) and Yin Guo for helpful discussions and Dr. Jeffrey P. Bond (UVM) for critical reading of the manuscript. This work was supported by National Institutes of Health grants P01 CA098993 to SSW and R01 CA090689 to CJB awarded by the National Cancer Institute.

References

1. Krokan HE, Standal R, Slupphaug G. DNA glycosylases in the base excision repair of DNA. Biochem J 1997;325(Pt 1):1–16. [PubMed: 9224623]

2. McCullough AK, Dodson ML, Lloyd RS. Initiation of base excision repair: glycosylase mechanisms and structures. Annu Rev Biochem 1999;68:255–285. [PubMed: 10872450]
3. Wallace SS, Bandaru V, Kathe SD, Bond JP. The enigma of endonuclease VIII. DNA Repair (Amst) 2003;2:441–453. [PubMed: 12713806]
4. David SS, Williams SD. Chemistry of Glycosylases and Endonucleases Involved in Base-Excision Repair. Chem Rev 1998;98:1221–1262. [PubMed: 11848931]
5. Hickerson RP, Chepanoske CL, Williams SD, David SS, Burrows CJ. Mechanism-Based DNA-Protein Cross-Linking of MutY via Oxidation of 8-Oxoguanosine (Communication). J Am Chem Soc 1999;121:9901–9902.
6. Goyal RN, Dryhurst G. Redox chemistry of guanine and 8-oxyguanine and a comparison of the peroxidase-catalyzed and electrochemical oxidation of 8-oxyguanine. J Electoranal Chem 1982;135:75–91.
7. Luo W, Muller JG, Rachlin EM, Burrows CJ. Characterization of spiroiminodihydantoin as a product of one-electron oxidation of 8-Oxo-7,8-dihydroguanosine. Org Lett 2000;2:613–616. [PubMed: 10814391]
8. Sugden KD, Martin BD. Guanine and 7,8-dihydro-8-oxo-guanine-specific oxidation in DNA by chromium(V). Environ Health Perspect 2002;110(Suppl 5):725–728. [PubMed: 12426120]
9. Duarte V, Muller JG, Burrows CJ. Insertion of dGMP and dAMP during in vitro DNA synthesis opposite an oxidized form of 7,8-dihydro-8-oxoguanine. Nucleic Acids Res 1999;27:496–502. [PubMed: 9862971]
10. Henderson PT, Delaney JC, Gu F, Tannenbaum SR, Essigmann JM. Oxidation of 7,8-dihydro-8-oxoguanine affords lesions that are potent sources of replication errors in vivo. Biochemistry 2002;41:914–921. [PubMed: 11790114]
11. Leipold MD, Muller JG, Burrows CJ, David SS. Removal of hydantoin products of 8-oxoguanine oxidation by the Escherichia coli DNA repair enzyme, FPG. Biochemistry 2000;39:14984–14992. [PubMed: 11101315]
12. Hazra TK, Muller JG, Manuel RC, Burrows CJ, Lloyd RS, Mitra S. Repair of hydantoins, one electron oxidation product of 8-oxoguanine, by DNA glycosylases of *Escherichia coli*. Nucleic Acids Res 2001;29:1967–1974. [PubMed: 11328881]
13. Gilboa R, Zharkov DO, Golan G, Fernandes AS, Gerchman SE, Matz E, Kycia JH, Grollman AP, Shoham G. Structure of formamidopyrimidine-DNA glycosylase covalently complexed to DNA. J Biol Chem 2002;277:19811–19816. [PubMed: 11912217]
14. Zharkov DO, Golan G, Gilboa R, Fernandes AS, Gerchman SE, Kycia JH, Rieger RA, Grollman AP, Shoham G. Structural analysis of an Escherichia coli endonuclease VIII covalent reaction intermediate. Embo J 2002;21:789–800. [PubMed: 11847126]
15. Jiang D, Hatahet Z, Melamede RJ, Kow YW, Wallace SS. Characterization of Escherichia coli endonuclease VIII. J Biol Chem 1997;272:32230–32239. [PubMed: 9405426]
16. Bandaru V, Sunkara S, Wallace SS, Bond JP. A novel human DNA glycosylase that removes oxidative DNA damage and is homologous to Escherichia coli endonuclease VIII. DNA Repair (Amst) 2002;1:517–529. [PubMed: 12509226]
17. Hazra TK, Izumi T, Boldogh I, Imhoff B, Kow YW, Jaruga P, Dizdaroglu M, Mitra S. Identification and characterization of a human DNA glycosylase for repair of modified bases in oxidatively damaged DNA. Proc Natl Acad Sci U S A 2002;99:3523–3528. [PubMed: 11904416]
18. Hazra TK, Kow YW, Hatahet Z, Imhoff B, Boldogh I, Mokkapati SK, Mitra S, Izumi T. Identification and characterization of a novel human DNA glycosylase for repair of cytosine-derived lesions. J Biol Chem 2002;277:30417–30420. [PubMed: 12097317]
19. Morland I, Rolseth V, Luna L, Rognes T, Bjoras M, Seeberg E. Human DNA glycosylases of the bacterial Fpg/MutM superfamily: an alternative pathway for the repair of 8-oxoguanine and other oxidation products in DNA. Nucleic Acids Res 2002;30:4926–4936. [PubMed: 12433996]
20. Takao M, Kanno S, Kobayashi K, Zhang QM, Yonei S, van der Horst GT, Yasui A. A back-up glycosylase in Nth1 knock-out mice is a functional Nei (endonuclease VIII) homologue. J Biol Chem 2002;277:42205–42213. [PubMed: 12200441]

21. Raoult D, Audic S, Robert C, Abergel C, Renesto P, Ogata H, La Scola B, Suzan M, Claverie JM. The 1.2-megabase genome sequence of Mimivirus. Science 2004;306:1344–1350. [PubMed: 15486256]
22. Bandaru V, Blaisdell JO, Wallace SS. Oxidative DNA glycosylases: recipes from cloning to characterization. Methods Enzymol 2006;408:15–33. [PubMed: 16793360]
23. Kornyushyna O, Berges AM, Muller JG, Burrows CJ. In vitro nucleotide misinsertion opposite the oxidized guanosine lesions spiroiminodihydantoin and guanidinohydantoin and DNA synthesis past the lesions using Escherichia coli DNA polymerase I (Klenow fragment). Biochemistry 2002;41:15304–15314. [PubMed: 12484769]
24. Garcia-Diaz M, Bebenek K, Kunkel TA, Blanco L. Identification of an intrinsic 5′-deoxyribose-5-phosphate lyase activity in human DNA polymerase lambda: a possible role in base excision repair. J Biol Chem 2001;276:34659–34663. [PubMed: 11457865]
25. Dou H, Mitra S, Hazra TK. Repair of oxidized bases in DNA bubble structures by human DNA glycosylases NEIL1 and NEIL2. J Biol Chem 2003;278:49679–49684. [PubMed: 14522990]
26. Hirel PH, Schmitter MJ, Dessen P, Fayat G, Blanquet S. Extent of N-terminal methionine excision from *Escherichia coli* proteins is governed by the side-chain length of the penultimate amino acid. Proc Natl Acad Sci U S A 1989;86:8247–8251. [PubMed: 2682640]
27. Frottin F, Martinez A, Peynot P, Mitra S, Holz RC, Giglione C, Meinnel T. The proteomics of N-terminal methionine cleavage. Mol Cell Proteomics 2006;5:2336–2349. [PubMed: 16963780]
28. Hailer MK, Slade PG, Martin BD, Rosenquist TA, Sugden KD. Recognition of the oxidized lesions spiroiminodihydantoin and guanidinohydantoin in DNA by the mammalian base excision repair glycosylases NEIL1 and NEIL2. DNA Repair (Amst) 2005;4:41–50. [PubMed: 15533836]
29. Graves RJ, Felzenszwalb I, Laval J, O'Connor TR. Excision of 5′-terminal deoxyribose phosphate from damaged DNA is catalyzed by the Fpg protein of Escherichia coli. J Biol Chem 1992;267:14429–14435. [PubMed: 1378443]
30. Zhang QM, Yonekura S, Takao M, Yasui A, Sugiyama H, Yonei S. DNA glycosylase activities for thymine residues oxidized in the methyl group are functions of the hNEIL1 and hNTH1 enzymes in human cells. DNA Repair (Amst) 2005;4:71–79. [PubMed: 15533839]
31. Kropachev KY, Zharkov DO, Grollman AP. Catalytic mechanism of *Escherichia coli* endonuclease VIII: roles of the intercalation loop and the zinc finger. Biochemistry 2006;45:12039–12049. [PubMed: 17002303]
32. Golan G, Zharkov DO, Grollman AP, Dodson ML, McCullough AK, Lloyd RS, Shoham G. Structure of T4 pyrimidine dimer glycosylase in a reduced imine covalent complex with abasic site-containing DNA. J Mol Biol 2006;362:241–258. [PubMed: 16916523]
33. Chen R, Wang H, Mansky LM. Roles of uracil-DNA glycosylase and dUTPase in virus replication. J Gen Virol 2002;83:2339–2345. [PubMed: 12237414]
34. Suzan-Monti M, La Scola B, Raoult D. Genomic and evolutionary aspects of *Mimivirus*. Virus Res 2006;117:145–155. [PubMed: 16181700]
35. Suhre K, Audic S, Claverie JM. Mimivirus gene promoters exhibit an unprecedented conservation among all eukaryotes. Proc Natl Acad Sci U S A 2005;102:14689–14693. [PubMed: 16203998]
36. Renesto P, Abergel C, Decloquement P, Moinier D, Azza S, Ogata H, Fourquet P, Gorvel JP, Claverie JM. Mimivirus giant particles incorporate a large fraction of anonymous and unique gene products. J Virol 2006;80:11678–11685. [PubMed: 16971431]
37. Ogata H, Abergel C, Raoult D, Claverie JM. Response to Comment on "The 1.2-Megabase Genome Sequence of Mimivirus". Science 2005;308:1114B. [PubMed: 15905382]
38. Greub G, Raoult D. Microorganisms resistant to free-living amoebae. Clin Microbiol Rev 2004;17:413–433. [PubMed: 15084508]
39. Claverie JM, Ogata H, Audic S, Abergel C, Suhre K, Fournier PE. Mimivirus and the emerging concept of "giant" virus. Virus Res 2006;117:133–144. [PubMed: 16469402]
40. Ghedin E, Claverie JM. Mimivirus relatives in the Sargasso sea. Virol J 2005;2:62. [PubMed: 16105173]
41. Schuster FL, Visvesvara GS. Free-living amoebae as opportunistic and non-opportunistic pathogens of humans and animals. Int J Parasitol 2004;34:1001–1027. [PubMed: 15313128]

42. Kadlec V. The occurrence of amphizoic Amebae in domestic animals. J Protozool 1978;25:235–237. [PubMed: 690954]
43. Sugahara M, Mikawa T, Kumasaka T, Yamamoto M, Kato R, Fukuyama K, Inoue Y, Kuramitsu S. Crystal structure of a repair enzyme of oxidatively damaged DNA, MutM (Fpg), from an extreme thermophile, Thermus thermophilus HB8. Embo J 2000;19:3857–3869. [PubMed: 10921868]
44. Doublié S, Bandaru V, Bond JP, Wallace SS. The crystal structure of human endonuclease VIII-like 1 (NEIL1) reveals a zincless finger motif required for glycosylase activity. Proc Natl Acad Sci U S A 2004;101:10284–10289. [PubMed: 15232006]
45. Das A, Rajagopalan L, Mathura VS, Rigby SJ, Mitra S, Hazra TK. Identification of a zinc finger domain in the human NEIL2 (Nei-like-2) protein. J Biol Chem 2004;279:47132–47138. [PubMed: 15339932]
46. Oliveros M, Yanez RJ, Salas ML, Salas J, Vinuela E, Blanco L. Characterization of an African swine fever virus 20-kDa DNA polymerase involved in DNA repair. J Biol Chem 1997;272:30899–30910. [PubMed: 9388236]
47. Lamarche BJ, Tsai MD. Contributions of an endonuclease IV homologue to DNA repair in the African swine fever virus. Biochemistry 2006;45:2790–2803. [PubMed: 16503634]
48. Benarroch D, Shuman S. Characterization of mimivirus NAD+-dependent DNA ligase. Virology 2006;353:133–143. [PubMed: 16844179]
49. Srivastava DK, Berg BJ, Prasad R, Molina JT, Beard WA, Tomkinson AE, Wilson SH. Mammalian abasic site base excision repair. Identification of the reaction sequence and rate-determining steps. J Biol Chem 1998;273:21203–21209. [PubMed: 9694877]
50. Piersen CE, Prasad R, Wilson SH, Lloyd RS. Evidence for an imino intermediate in the DNA polymerase beta deoxyribose phosphate excision reaction. J Biol Chem 1996;271:17811–17815. [PubMed: 8663612]
51. Grin IR, Khodyreva SN, Nevinsky GA, Zharkov DO. Deoxyribophosphate lyase activity of mammalian endonuclease VIII-like proteins. FEBS Lett 2006;580:4916–4922. [PubMed: 16920106]

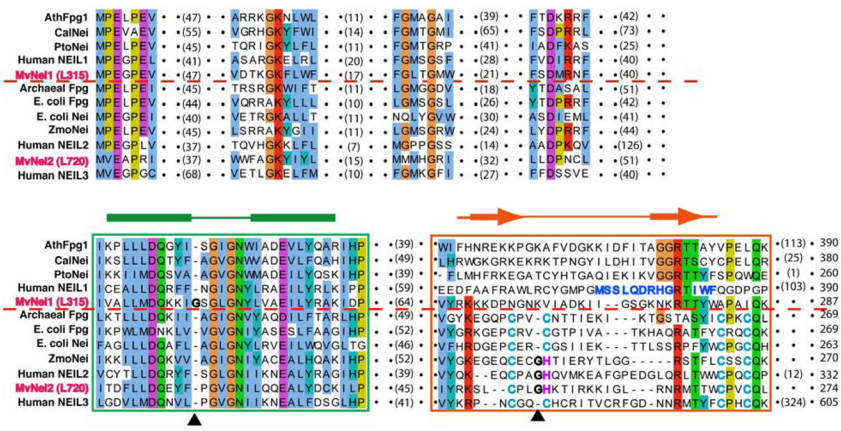

Fig. 1. Sequence alignment of endonuclease VIII-like proteins (NEIL) with the representative members of Fpg/Nei family

Numbers in parenthesis represent residues not shown between the regions. For MvNei2, the N-terminal 43 aa extension is not shown. The conserved proline and arginine residues important for the DNA glycosylase activity of Fpg/Nei members are denoted by an asterix. Positions where residues are inserted in MvNei1, MvNei2, ZmoNei and NEIL2 are shown by a filled triangle (▲). The DNA binding helix-two turns-helix (H2TH) motif and the β-hairpin loop of the zinc finger motif are boxed in green and orange respectively. The "zincless finger" motif in human NEIL1 is highlighted in blue. The four cysteines that coordinate the zinc atom are shown in cyan except for ZmoNei, MvNei2 and human NEIL2 where the second cysteine is replaced by a histidine colored purple. Dashed redline demarcates "zincless finger" from zinc finger-containing proteins. AtFpg1: *Arabidopsis thaliana* MMH-1 (gi|18404050); CalNei: *Candida albicans* Nei (gi|3850130); PtoNei: *Psychroflexus torquis* Nei (gi|91215880); human NEIL1 (gi|13375817); MvNei1: Mimivirus Nei1 (gi|55819191); Archaeal Fpg (gi|56295548); *E. coli* Fpg (gi|16131506); *E. coli* Nei (gi|16128689); ZmoNei: *Zymomonas mobilis* Nei (gi|56552083); human NEIL2 (gi|21450800); MvNei2: Mimivirus Nei2 (gi|55819586) and human NEIL3 (gi|19684059).

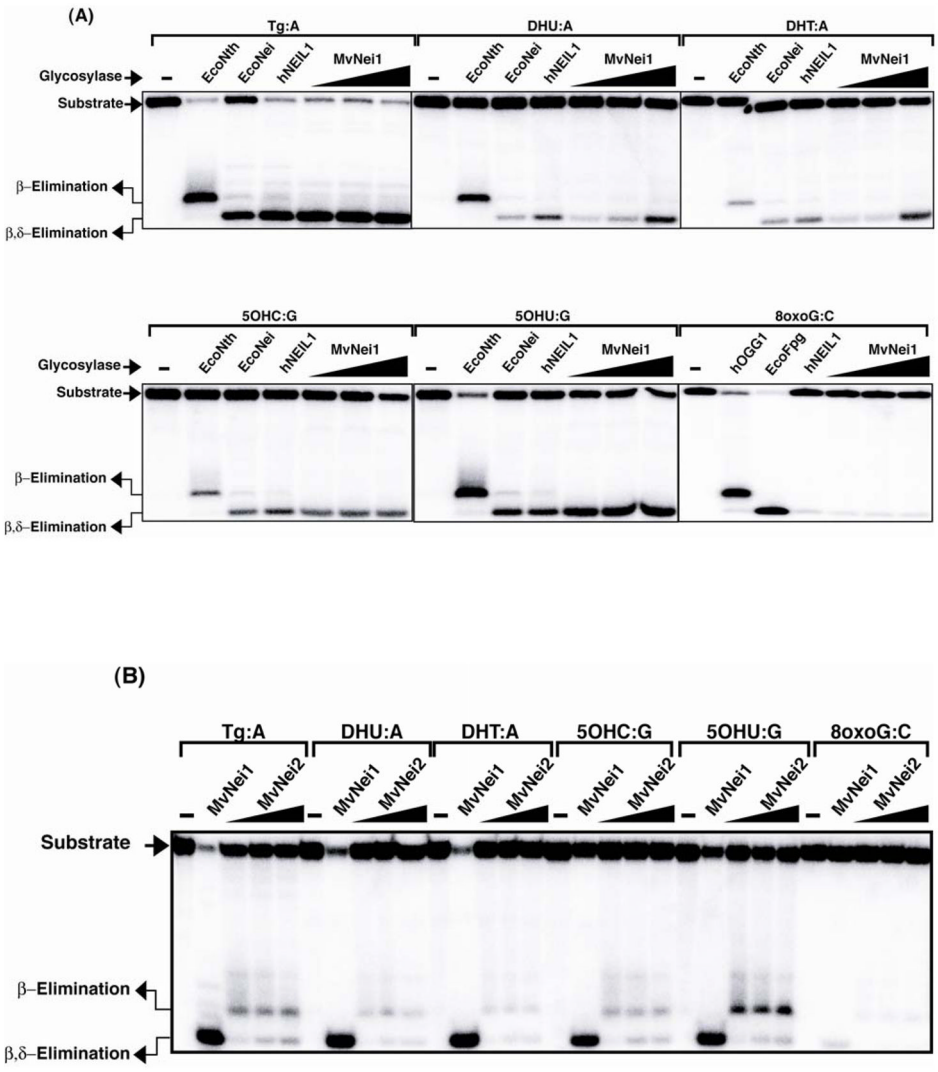

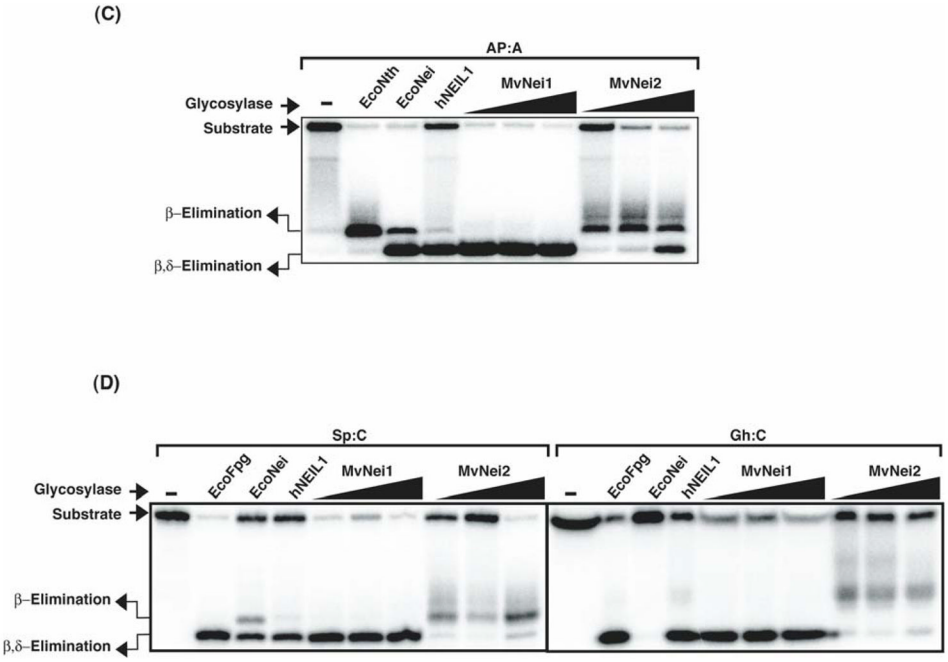

Fig. 2. DNA glycosylase/lyase activities of mimiviral Nei proteins

A and *B*, Substrate specificity of MvNei1 and MvNei2 for oxidative DNA damages. *C*, Activity of MvNei1 and 2 on guanidinohydantoin (Gh) and spiroiminodihydantoin (Sp) substrates. *D*, Lyase activity of MvNei1 and 2 on an AP substrate. For panels A, C and D, ^{32}P-labeled substrates (25 nM) were incubated with 50 nM of EcoNth, EcoNei, human NEIL1, CalNei, EcoFpg, hOGG1 and increasing concentrations of (50 nM, 125 nM and 250 nM) of MvNei1 and MvNei2 in their respective assay buffers as described in “Experimental Procedures”. In Panel B, 25 nM labeled substrate was incubated with 50 nM MvNei1 and varying concentrations (100 nM, 250 nM and 1.25 μM) of MvNei2. The reaction volumes were normalized to radioactive counts before loading onto a denaturing PAGE gel.

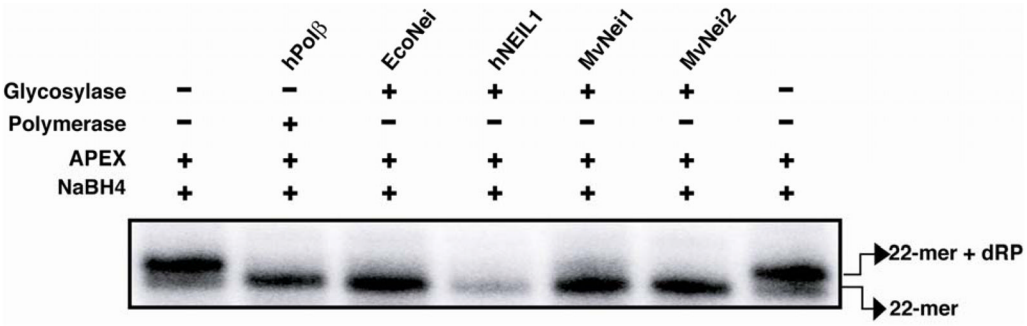

Fig. 3. dRPase activity of MvNei1 and 2

A 22-mer substrate containing a 5′-dRP moiety was prepared as described under "Experimental Procedures". Substrate (10 nM) was treated with 100 nM of EcoNei, human NEIL1, MvNei1 and MvNei2 or 1 unit of human DNA polymerase β. Unreacted 22-mer containing 5′-dRP was stabilized by reducing with $NaBH_4$ and analyzed on a denaturing PAGE gel.

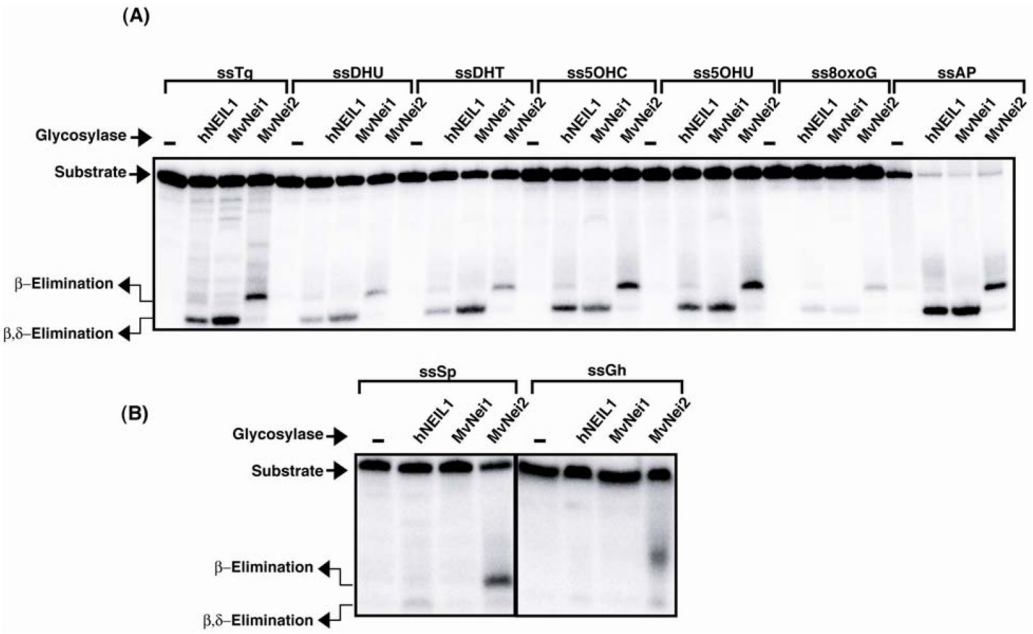

Fig. 4. Specificities of MvNei1 and 2 for oxidized DNA damages in single stranded DNA

Radioactivly labeled single stranded damage-containing oligonucleotides (25 nM) were incubated at 37°C with 25 nM human NEIL1, MvNei1 and MvNei2 in their respective assay buffers as described in “Experimental Procedures”

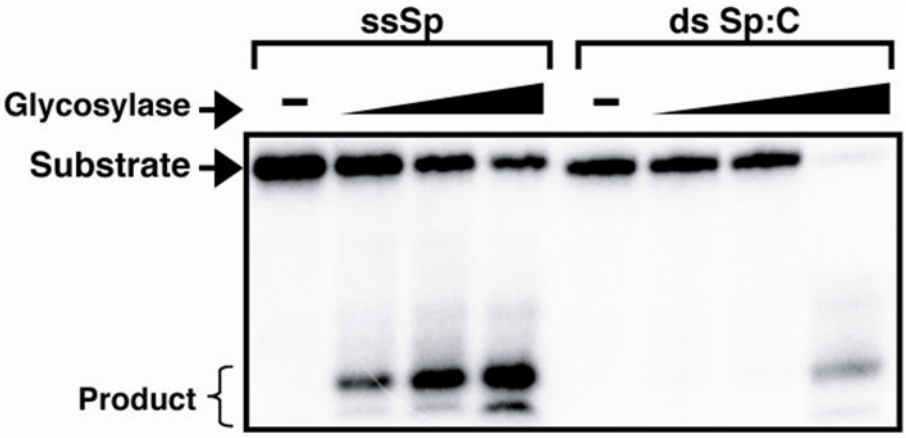

Fig. 5. Differential activity of MvNei2 on single and double stranded DNA substrates

MvNei2 (50 nM, 125 nM and 250 nM) was incubated with 25 nM of 5′end labeled single stranded spiroiminodihydantoin (Sp) oligonucleotide and 25 nM of double stranded Sp:C substrate at 37°C for 30 min.

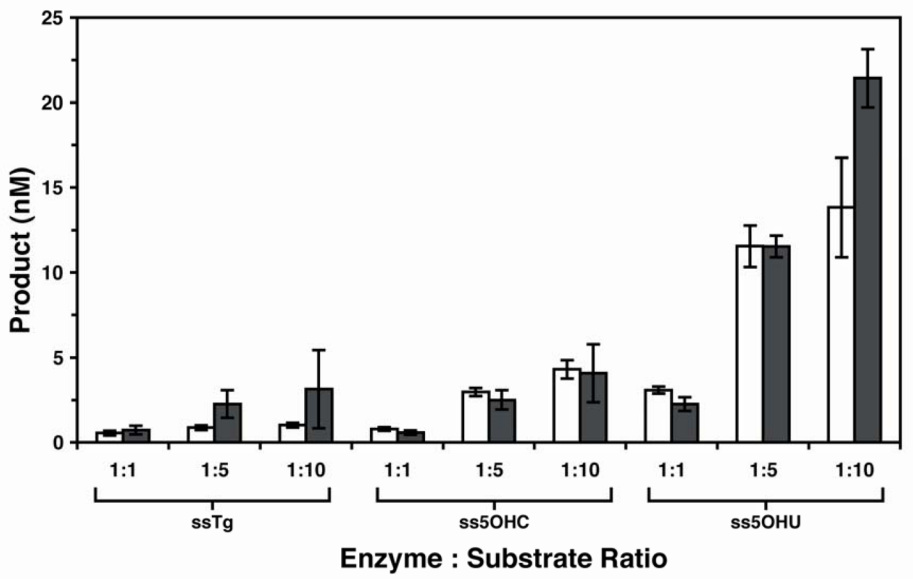

Fig. 6. Activities of human NEIL1 and MvNei1 on single stranded oligonucleotides containing oxidative lesions

10 nM human NEIL1 (empty) or MvNei1 (filled) was incubated with 10 nM, 50 nM and 100 nM single stranded substrates at 37°C for 30 min. Error bars represent standard error of the mean from 3 separate experiments.

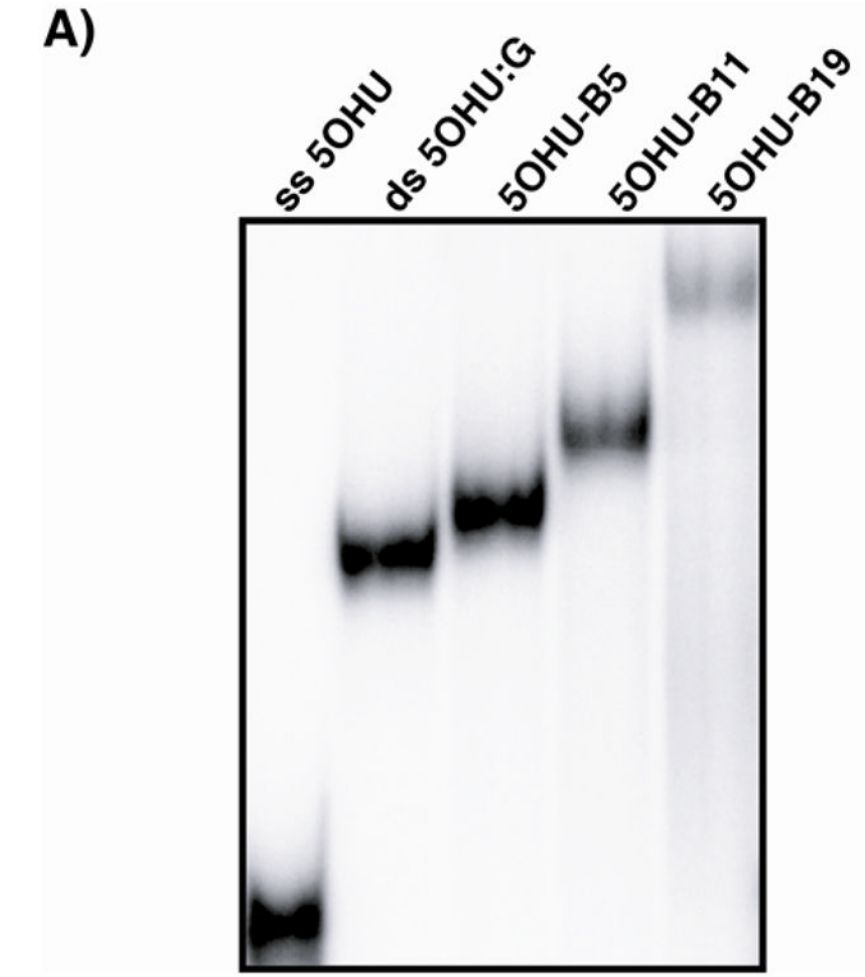

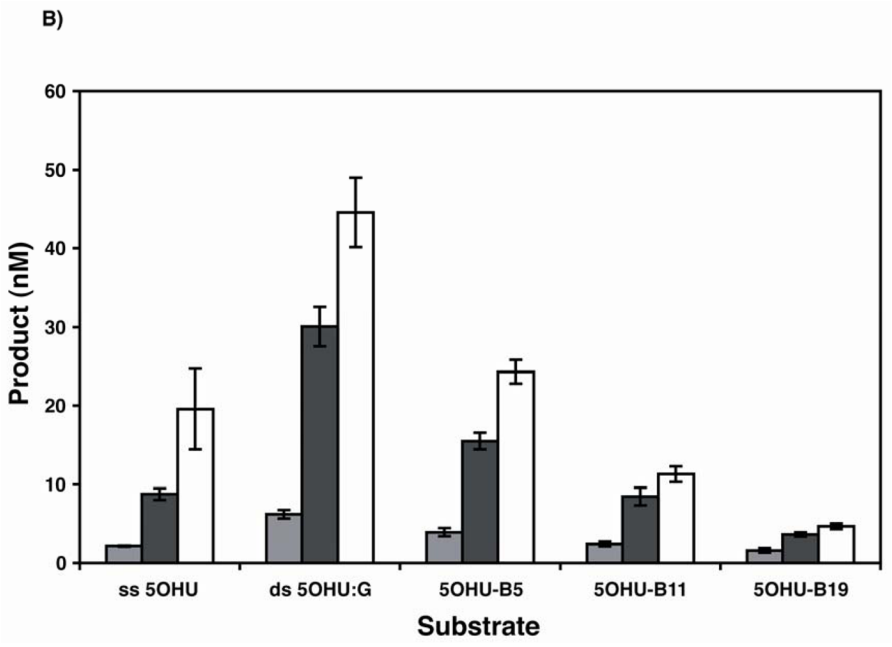

Fig. 7. Activity of MvNei1 on damage-containing bubble substrates

A, Substrates with 5OHU in single stranded DNA (ss5OHU), duplex DNA (ds5OHU) or in various size bubbles (B5, B11, B19) were prepared as described under “Experimental Procedures” and analyzed on a 10% native PAGE gel to verify the secondary structure in the substrates. *B,* 10 nM (filled), 50 nM (gray) or 100 nM (empty) single stranded, double stranded or bubble substrates containing the 5OHU damage were incubated with 10 nM enzyme as described under “Experimental Procedures”. Error bars represent standard error of the mean from 3 separate experiments.

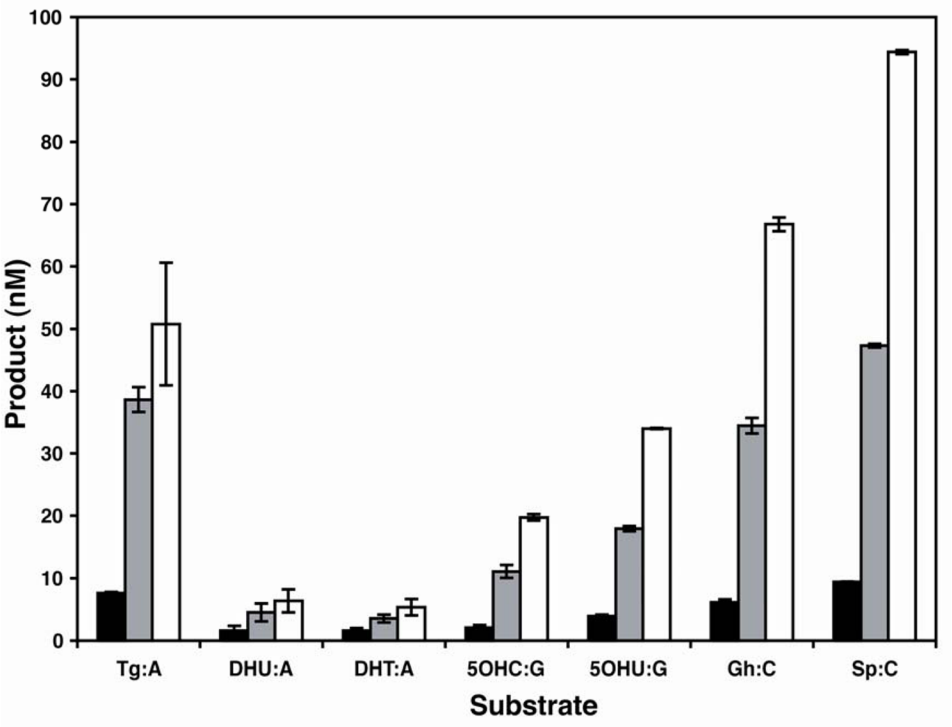

Fig. 8. Substrate specificity of MvNei1 under steady state conditions

10 nM (black), 50 nM (gray) and 100 nM (empty) of radiolabeled double stranded substrates containing various base damages were incubated with 10 nM MvNei1 at 37°C for 30 min. Error bars represent standard error of the mean from 3 separate experiments.

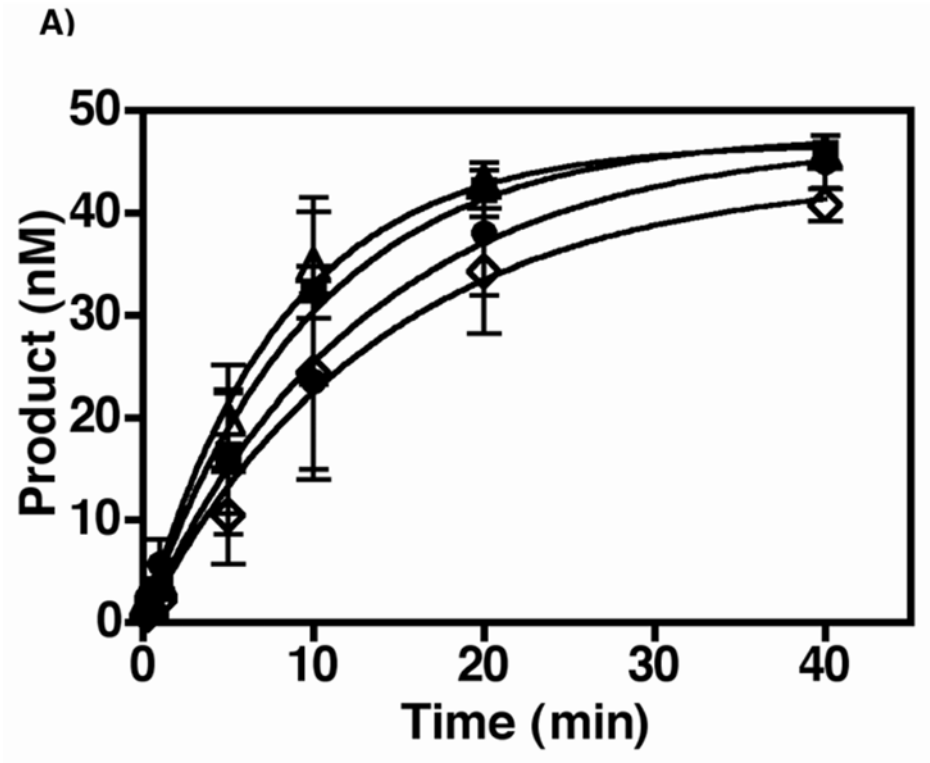

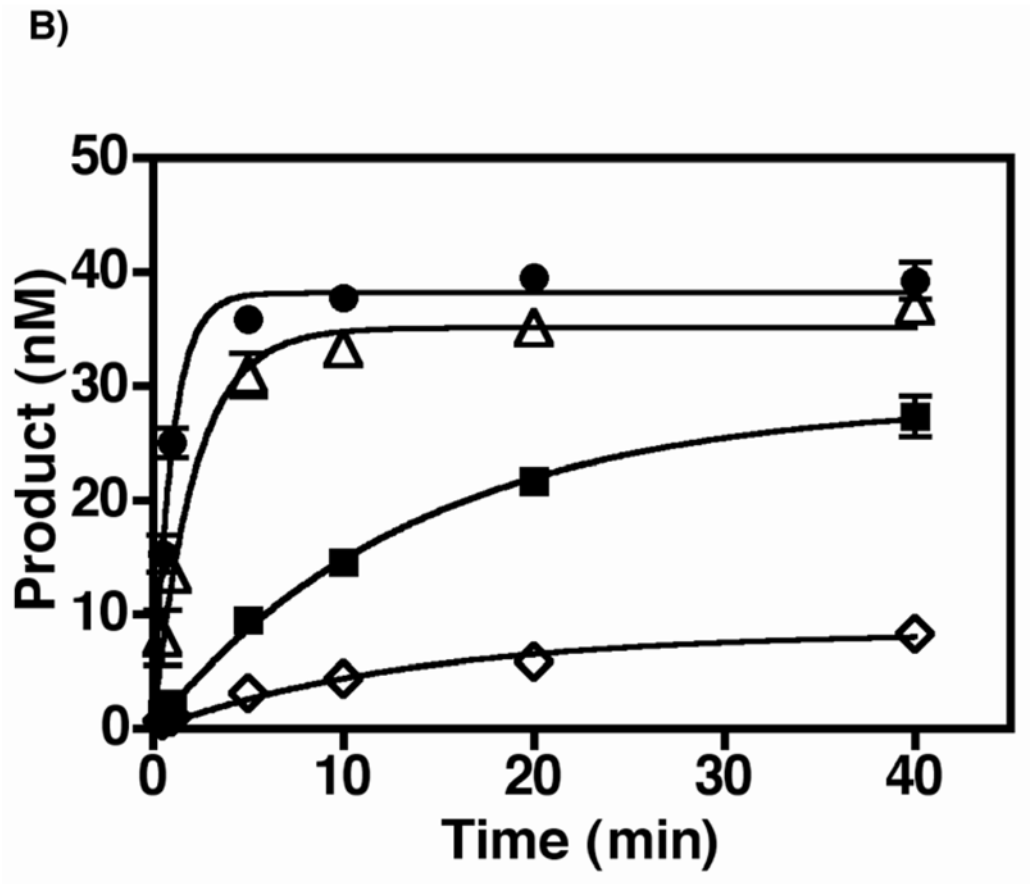

Fig. 9. Opposite base specificity of MvNei1

10 nM MvNei1 was incubated with 50 nM substrate with A (◇), T (■), G(△), C (●) bases opposite *A*, thymine glycol (Tg) and *B*, guanidinohydantoin (Gh) damages at 37°C for various times. Error bars represent standard error of the mean from 3 separate experiments.

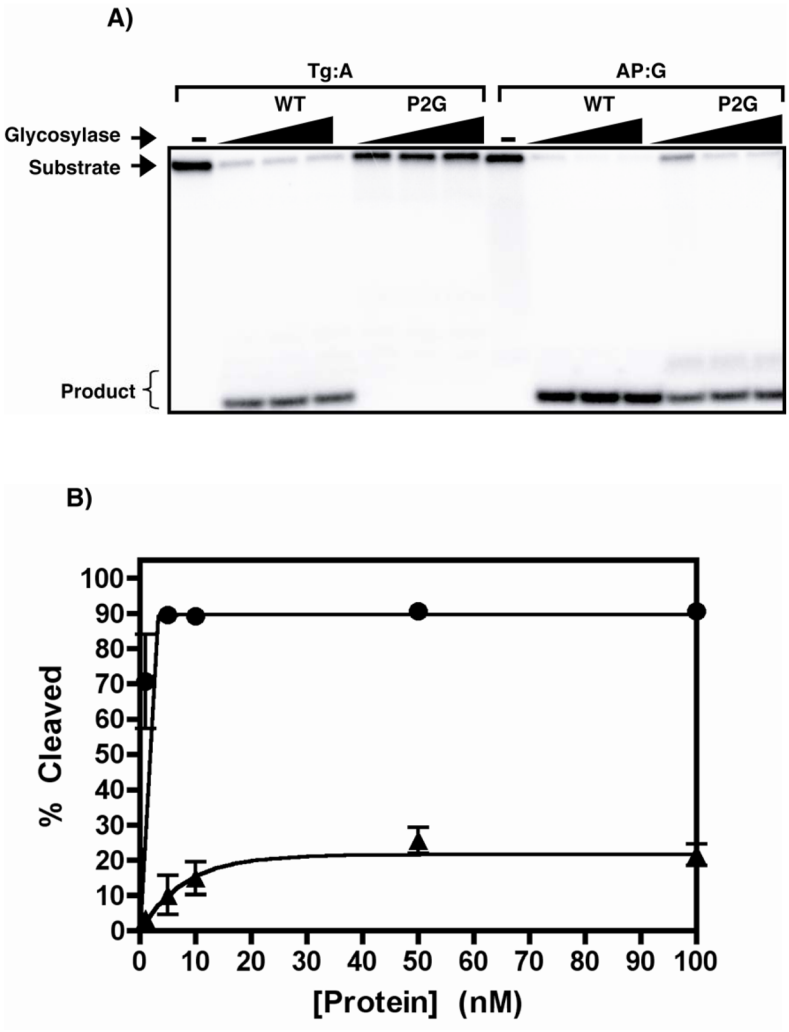

Fig. 10. DNA glycosylase/lyase activities of wild type and mutant MvNei1

A, Radiolabeled Tg:A and AP:G substrates (25 nM) were incubated with 25 nM, 125 nM and 250 nM wild type and mutant MvNei1 enzymes as described under "Experimental Procedures". *B*, Effect of R277A mutation on the DNA glycosylase/lyase activity on a Tg:A substrate. 10 nM radiolabeled substrate was incubated with different concentrations of wild type (●) and R277A mutant (▲) as described under "Experimental Procedures". Error bars represent standard error of the mean from 3 separate experiments.

Table 1

Kinetic parameters of MvNei1 for duplex DNA substrates.

Substrate	K_m (nM)	K_{cat} (sec^{-1})	K_{cat}/K_m (sec^{-1} nM^{-1})
Tg:A	2.33	1.42	0.6
Gh-C	1.3	19	14.6
Gh-A	1100	19.4	0.02